AMERICAN SOCIETY FOR MICROBIOLOGY | mBio®

RESEARCH ARTICLE

# Mitochondrial Cochaperone Mge1 Is Involved in Regulating Susceptibility to Fluconazole in *Saccharomyces cerevisiae* and *Candida* Species

**Liesbeth Demuyser,[a,b] Erwin Swinnen,[a,b,c] Alessandro Fiori,[a,b]* Beatriz Herrera-Malaver,[a,d] Kevin Verstrepen,[a,d] Patrick Van Dijck[a,b]**

VIB-KU Leuven Center for Microbiology, Flanders, Belgium[a]; Laboratory of Molecular Cell Biology, Institute of Botany and Microbiology, KU Leuven, Leuven, Belgium[b]; Laboratory of Functional Biology, Institute of Botany and Microbiology, KU Leuven, Leuven, Belgium[c]; Laboratory for Genetics and Genomics, KU Leuven, Leuven, Belgium[d]

**ABSTRACT** *MGE1* encodes a yeast chaperone involved in Fe-S cluster metabolism and protein import into the mitochondria. In this study, we identified *MGE1* as a multicopy suppressor of susceptibility to the antifungal fluconazole in the model yeast *Saccharomyces cerevisiae*. We demonstrate that this phenomenon is not exclusively dependent on the integrity of the mitochondrial DNA or on the presence of the drug efflux pump Pdr5. Instead, we show that the increased dosage of Mge1 plays a protective role by retaining increased amounts of ergosterol upon fluconazole treatment. Iron metabolism and, more particularly, Fe-S cluster formation are involved in regulating this process, since the responsible Hsp70 chaperone, Ssq1, is required. Additionally, we show the necessity but, by itself, insufficiency of activating the iron regulon in establishing the Mge1-related effect on drug susceptibility. Finally, we confirm a similar role for Mge1 in fluconazole susceptibility in the pathogenic fungi *Candida glabrata* and *Candida albicans*.

**IMPORTANCE** Although they are mostly neglected compared to bacterial infections, fungal infections pose a serious threat to the human population. While some of them remain relatively harmless, infections that reach the bloodstream often become lethal. Only a few therapies are available, and resistance of the pathogen to these drugs is a frequently encountered problem. It is thus essential that more research is performed on how these pathogens cope with the treatment and cause recurrent infections. Baker's yeast is often used as a model to study pathogenic fungi. We show here, by using this model, that iron metabolism and the formation of the important iron-sulfur clusters are involved in regulating susceptibility to fluconazole, the most commonly used antifungal drug. We show that the same process likely also occurs in two of the most regularly isolated pathogenic fungi, *Candida glabrata* and *Candida albicans*.

**KEYWORDS** *Candida albicans*, *Candida glabrata*, Fe-S cluster, Mge1, *Saccharomyces cerevisiae*, antifungal susceptibility, fluconazole, iron metabolism, mitochondrial chaperone

**Received** 22 May 2017 **Accepted** 15 June 2017 **Published** 18 July 2017

**Citation** Demuyser L, Swinnen E, Fiori A, Herrera-Malaver B, Verstrepen K, Van Dijck P. 2017. Mitochondrial cochaperone Mge1 is involved in regulating susceptibility to fluconazole in *Saccharomyces cerevisiae* and *Candida* species. mBio 8:e00201-17. https://doi.org/10.1128/mBio.00201-17.

**Editor** J. Andrew Alspaugh, Duke University Medical Center



Address correspondence to Patrick Van Dijck, patrick.vandijck@kuleuven.vib.be.

* Present address: Alessandro Fiori, Agrosavfe NV, Ghent, Belgium.

Fungal infections pose a significant threat to the health of humans and other organisms. Some of these infections are superficial and merely impose a mild form of inconvenience to the patient, while others are invasive, causing severe disease and, potentially, death. Once an invasive infection is established, the likelihood of survival for the patient rarely exceeds 50% (1). The gravity of fungal infections and the concomitant importance of searching for new and better antifungal therapies are

generally underappreciated. The number of drugs available against fungal infections is limited, and those that are commonly used often suffer from being fungistatic rather than fungicidal (2, 3). The azoles, with fluconazole (flu) being the most studied, comprise one of these commonly used, fungistatic classes of antifungals (4). The azoles target the ergosterol biosynthesis pathway, more particularly, the lanosterol 14$\alpha$-demethylase (Erg11). This enzyme is essential in *Saccharomyces cerevisiae*, making the nonfungicidal nature of these drugs paradoxical (5, 6). Resistance to azoles is regularly caused by increased expression of genes encoding efflux pumps, causing overexpression of or altering the target gene by point mutations or generating cellular responses to cope with stress (4). The fungus can, however, also obtain certain transient, metabolic or epigenetic, adaptations that confer decreased susceptibility to the antifungal agent. This slow residual growth at inhibitory concentrations of the drug is called tolerance or trailing growth and hypothetically also generates the time needed for and the possibility of directional selection promoting the acquirement of alterations in the genome, causing resistance (7, 8).

In this project, we isolated *MGE1* as a multicopy suppressor of fluconazole susceptibility in *S. cerevisiae*. Mge1 is a cochaperone for members of the Hsp70 family of chaperones (9, 10), which serve functions in several cellular processes such as protein folding, preventing protein aggregation, protein translocation, targeted degradation, and adjusting the activity of regulatory proteins (11, 12). This cochaperone was discovered as a member of the mitochondrial import system, translocating proteins across the inner membrane into the matrix of the mitochondria (9, 13–15). The Hsp70 molecule involved is Ssc1, which is, like Mge1, an essential protein and is involved in refolding of denatured proteins (9, 16–18). Mge1 also functions as the nucleotide exchange factor of Ssq1, another Hsp70 chaperone, which is involved in the Fe-S cluster biosynthesis pathway (19). Fe-S clusters are essential cofactors involved in redox, catalytic, and regulatory processes, including the regulation of the iron starvation response (20–24). Ssq1 is responsible for transferring the assembled Fe-S cluster from the Isu1 scaffold to the target protein by destabilizing the connection between the cluster and this scaffold (25). In contrast to Ssc1 and Mge1, Ssq1 is not essential because when Ssq1 is depleted, Ssc1 can probably take over part of its function (26). We showed earlier that iron metabolism is involved in regulating susceptibility to fluconazole, since addition of the iron chelator doxycycline to fluconazole-treated *Candida albicans* and *S. cerevisiae* cells reduces or even completely abolishes tolerance (7, 27). In this paper, we provide evidence of the involvement of Fe-S cluster metabolism and signaling through the iron regulon in the Mge1-dependent regulation of fluconazole susceptibility in *S. cerevisiae*. We also demonstrate that this altered susceptibility is accompanied by modulation of the metabolic flux through the ergosterol synthesis pathway. Finally, we show that overexpressing the orthologues of *MGE1* in the pathogenic fungi *C. glabrata* and *C. albicans* affects fluconazole susceptibility in a similar way. As such, elucidating this apparently conserved fungal mechanism may yield interesting new targets for drug development.

## RESULTS

**Increased dosage of Mge1 acts as a suppressor of susceptibility to fluconazole in *S. cerevisiae*.** Aiming to identify new regulators of fluconazole susceptibility, we performed a screening of BY4742 transformed with multicopy plasmids, containing parts of the *S. cerevisiae* genomic library obtained from F. Lacroute (28). To reduce the background growth of the reference strain on the screening medium containing supra-minimum inhibitory concentrations (MICs) of fluconazole, we added the iron chelator doxycycline, for which we and others reported a synergistic effect with fluconazole earlier (7, 27). The resulting reduction of background growth allowed us to more clearly distinguish true multicopy suppressors of fluconazole susceptibility. Using these sensitized screening conditions (10 $\mu$g/ml fluconazole and 50 $\mu$g/ml doxycycline), we isolated the Hsp70 cochaperone Mge1, next to Erg11, as a dosage-dependent suppressor of susceptibility to fluconazole. We subcloned the *MGE1* fragment (contain-

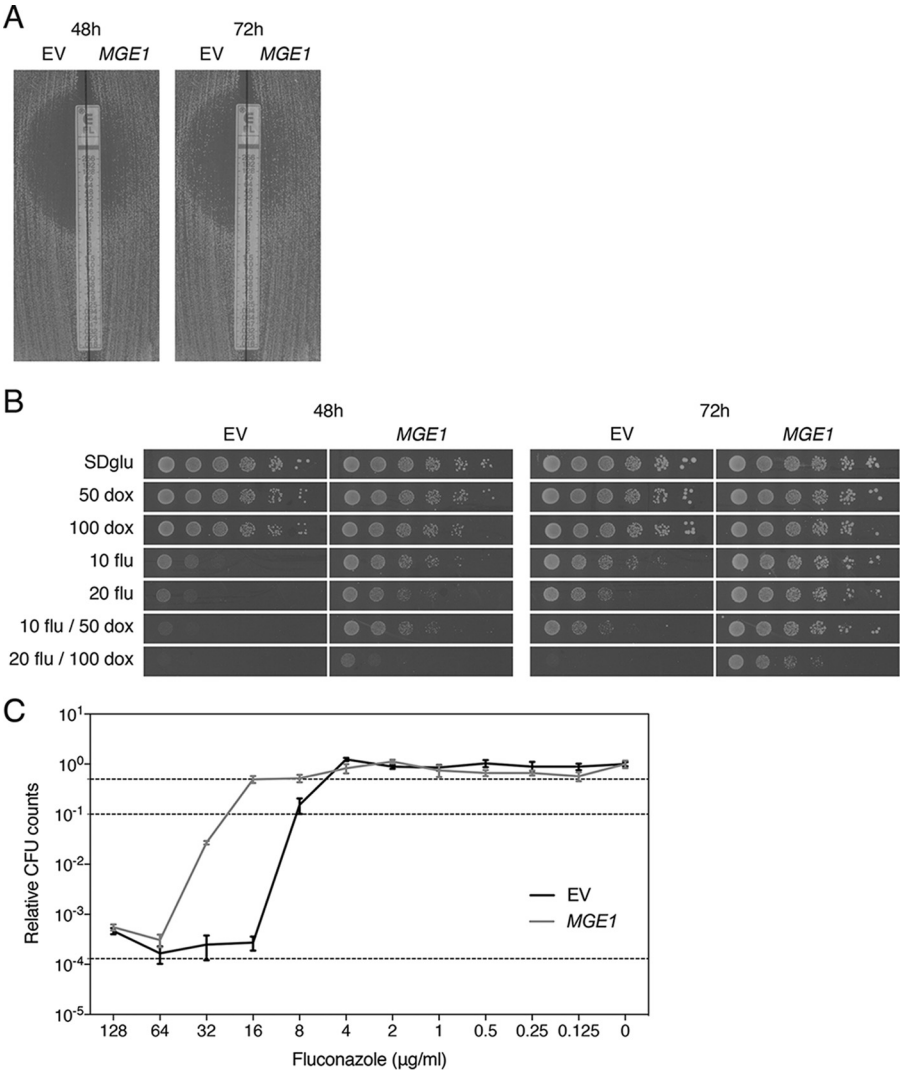


**FIG 1** *MGE1* overexpression improves growth of the wild-type *S. cerevisiae* strain on fluconazole. (A) Etest analysis of the overexpression strain (*MGE1*) and control strain (EV). (B) Serial dilutions of both strains were spotted on SDglu medium containing fluconazole (flu; 10 or 20 $\mu$g/ml) and/or doxycycline (dox; 50 or 100 $\mu$g/ml). Pictures were taken after 48 and 72 h of incubation at 30°C. (C) Tolerance assay. Data represent dose-response curves determined for both strains, with dotted lines indicating 50% (upper line) and 90% (middle line) growth inhibition and the initial inoculum (lower line). No significant difference was observed in trailing growth between the overexpression strain and control strain ($P = 0.731$ for 128 $\mu$g/ml flu and $P = 0.381$ for 64 $\mu$g/ml flu, tested by two-way ANOVA with Bonferroni correction).

ing the promoter, open reading frame [ORF], and terminator) from the pFL44 plasmid into YEPlac195 and verified overexpression in transformants using quantitative reverse transcription-PCR (qRT-PCR), which yielded a fold increase of 11.7 (standard error of the mean [SEM], 1.40) compared to the control strain. This increased expression causes a strong decrease in susceptibility to fluconazole compared to the empty vector control. The improved growth of the transformed BY4742 strain (indicated as *MGE1* in all figures) compared to the control (with empty YEPlac195, indicated as EV) was visualized by means of the Etest method and spot assays (Fig. 1A and B). The $MIC_{flu}$ of these strains was determined by Etest analyses and broth microdilution assays. All experiments were done with at least three biological repeats, showing consistent results. The $MIC_{flu}$ values are depicted in Table 1. We can conclude from these data that overexpression of *MGE1* causes a decrease in the susceptibility to fluconazole in *S. cerevisiae* and that this effect is more clearly visible under sensitized conditions where doxycycline is added to the medium. From the broth microdilution assay, we not only were

**TABLE 1** The effect of *MGE1* overexpression on the $MIC_{flu}$ of several strains[d]

| | $MIC_{flu}$ (μg/ml) | | |
|---|---|---|---|
| | | Broth microdilution assay | |
| Strain | Etest | $MIC_{50}$ | $MIC_{90}$ |
| *S. cerevisiae* BY4742 EV | 6–8 | 8–16 | 16 |
| *S. cerevisiae* BY4742 *MGE1* | 24–32 | 16–32 | 32–64 |
| *S. cerevisiae ira2*Δ EV | 4–6 | 8–16 | 8–16 |
| *S. cerevisiae ira2*Δ *MGE1* | 12–16 | 16–32 | 16–32 |
| *S. cerevisiae yme1*Δ EV | 12–16 | 8–16 | 16–32 |
| *S. cerevisiae yme1*Δ *MGE1* | 32–48 | 16–32 | 32–64 |
| *S. cerevisiae opi1*Δ EV | 12–16 | 8–16 | 8–16 |
| *S. cerevisiae opi1*Δ *MGE1* | 48–64 | 32–64 | 32–64 |
| *S. cerevisiae* rho$^0$ EV | 24–32 | 16–32 | 16–32 |
| *S. cerevisiae* rho$^0$ *MGE1* | >256 | 32–64 | 32–64 |
| *S. cerevisiae pdr5*Δ EV | 0.25 | 0.5–1 | 0.5–1 |
| *S. cerevisiae pdr5*Δ *MGE1* | 0.75 | 0.5–1 | 1–2 |
| *S. cerevisiae upc2*Δ EV | 4–6 | 4–8 | 4–8 |
| *S. cerevisiae upc2*Δ *MGE1* | 24–32 | 8–16 | 16–32 |
| *S. cerevisiae tom70*Δ EV | 6–8 | 8–16 | 8–16 |
| *S. cerevisiae tom70*Δ *MGE1* | 16–24 | 16–32 | 32–64 |
| *S. cerevisiae ecm10*Δ EV | 6–8 | 8–16 | 16–32 |
| *S. cerevisiae ecm10*Δ *MGE1* | 24–32 | 32–64 | 32–64 |
| *S. cerevisiae ssq1*Δ EV | 2–4[a] | 2–4[a] | 2–4[a] |
| *S. cerevisiae ssq1*Δ *MGE1* | 1–1.5[a] | —[b] | —[b] |
| *S. cerevisiae aft1*Δ EV | 4–6 | 8–16 | 16 |
| *S. cerevisiae aft1*Δ *MGE1* | 4–6 | 8–16 | 8–16 |
| *S. cerevisiae aft2*Δ EV | 4–6 | 8–16 | 8–16 |
| *S. cerevisiae aft2*Δ *MGE1* | 32–48 | 16–32 | 32–64 |
| *S. cerevisiae* BY4742 | 6–8 | 8–16 | 16–32 |
| *S. cerevisiae fra1*Δ | 6–8 | 8–16 | 16–32 |
| *C. glabrata* HTL EV | 8 (16–24)[c] | 2–4 | 4–8 |
| *C. glabrata* HTL *pTDH3-CgMGE1* | 24 (48–64)[c] | 4–8 | 8–16 |
| *C. glabrata* HTL *pPGK1-CgMGE1* | 16 (48–64)[c] | 2–4 | 8–16 |

[a]Data were determined after 72 h on SCglu (latter only for Etest).
[b]—, data could not be determined due to low growth.
[c]RPMI medium with 0.2% (or 2%) glucose was used.
[d]Values were determined by Etest and broth microdilution analysis. *MGE1*, *MGE1* overexpression; EV, empty vector control.

able to determine the $MIC_{50}$ and $MIC_{90}$ of the mutant compared to the control but also defined the effect of the overexpression on the growth at supra-MICs of fluconazole, called tolerance. Figure 1C shows that, although the $MIC_{50}$ and $MIC_{90}$ change clearly when *MGE1* is overexpressed, there is no significant difference between the colony forming unit (CFU) counts at higher fluconazole concentrations. Therefore, in the following parts of this article, we use only the $MIC_{flu}$ as a readout of drug susceptibility.

Next, we aimed to check the effect of fluconazole on *MGE1* expression under our experimental conditions. We performed qRT-PCR experiments on a wild-type BY4742 strain in the absence or presence of 20 μg/ml fluconazole. The expression of the gene decreased 2-fold in the presence of the drug, indicating that Mge1 itself might be a direct or indirect target of fluconazole {relative expression level with SEM, $1 \pm 0.046$ versus $0.498 \pm 0.045$ for 0 versus 20 μg/ml fluconazole with $P = <0.001$ [paired Student's *t* test on $\log_2(Y)$ transformed data]}.

**Mge1 can induce fluconazole resistance independently of rho$^0$ formation and Pdr5.** *S. cerevisiae* cells can lose part or all of their mitochondrial genome, generating so-called rho$^-$ or rho$^0$ cells, respectively (29, 30). It has been reported that such cells acquire resistance to certain chemicals such as fluconazole, though the underlying mechanisms are not yet fully known (31). Petite-negative strains contain nuclear mutations that render the loss of (part of) the mitochondrial genome lethal (32). Consequently, these strains cannot form rho$^0$ or rho$^-$ cells. To verify whether decreased fluconazole susceptibility of the *MGE1* overexpression strain might be caused by

increased generation of rho$^{0/-}$ cells, we transformed petite-negative strains with the overexpression vector. We chose three mutants involved in seemingly independent processes. The null mutants of *OPI1*, *IRA2*, and *YME1* were all discovered to be dependent on mitochondrial DNA (mtDNA) (33, 34). For these strains, the $MIC_{flu}$ tests were performed in minimal synthetic defined glucose (SDglu) medium as well as rich yeast extract-peptone-dextrose (YPD) medium, as it has been suggested that some petite-negative strains depend only on their mtDNA in rich medium (34). Figure S1A in the supplemental material and the $MIC_{flu}$ values in Table 1 and in Table S4 in the supplemental material show the sustained effect of *MGE1* overexpression on growth of the petite-negative strains in the presence of fluconazole, arguing against the hypothesis that rho$^{0/-}$ cells are the sole cause of improved growth on fluconazole. We have to take into account, however, that overexpression of *MGE1* could potentially suppress the dependency of the petite-negative mutants on their mtDNA. Nevertheless, overexpression of *MGE1* also causes an increase in the $MIC_{flu}$ of a rho$^0$ strain, as can be seen in Table 1 and Fig. S1A, confirming our hypothesis more incontestably. Taken together, these data suggest that the decreased susceptibility to fluconazole in *MGE1*-overexpressing cells is not (solely) caused by increased generation of rho$^{0/-}$ cells.

Overexpression of genes encoding drug efflux pumps is another well-known method of acquiring resistance to drugs that can penetrate the cell. In *Candida* species, expression of genes of the CDR and MDR families, encoding ABC transporters and major facilitators, respectively, are often found upregulated in clinically isolated resistant strains (35–37). The orthologue of the *C. albicans CDR1* gene in *S. cerevisiae* is *PDR5*. It was verified that *PDR5* expression is augmented in rho$^{0/-}$ cells compared to rho$^+$ cells. The acquired resistance to several types of chemicals is thought to be caused by this phenomenon (31). Expression levels of *PDR5* were higher in the *MGE1* overexpression strain, indicating that Pdr5 might have been involved in the increased growth on fluconazole {relative expression level $\pm$ SEM for 0 $\mu$g/ml fluconazole and EV versus *MGE1*, 1.000 $\pm$ 0.047 versus 1.596 $\pm$ 0.165 with $P < 0.01$; for 20 $\mu$g/ml fluconazole and EV versus *MGE1*, 1.482 $\pm$ 0.086 versus 2.494 $\pm$ 0.088 with $P < 0.001$ [Bonferroni-corrected two-way analysis of variance (ANOVA) of $\log_2$(Y) transformed data]}. To determine whether this increase was the sole cause of the decreased susceptibility of the *MGE1* overexpression strain, we assessed the effect of *MGE1* overexpression on the $MIC_{flu}$ of the *pdr5*$\Delta$ strain. It can be seen from Table S4 and Fig. S1B that deletion of *PDR5* in the rho$^0$ background reduced the $MIC_{flu}$ to the same level as deletion of *PDR5* in the wild-type BY4742 background, reinforcing the notion that much of the fluconazole resistance of rho$^{0/-}$ cells is due to upregulation of *PDR5* expression. Overexpressing *MGE1* in a *pdr5*$\Delta$ strain still resulted in a significant increase of the $MIC_{flu}$ from 0.25 to 0.75 $\mu$g/ml (Table 1; Fig. S1B) indicating that, while increased expression of *PDR5* in cells with an elevated dosage of Mge1 may still play a minor role, Mge1 can induce fluconazole resistance independently of the efflux pump.

**Overexpression of *MGE1* increases the residual amount of ergosterol after treatment with fluconazole independently of the expression of fluconazole-induced *ERG* genes.** As already shown by Arthington-Skaggs et al. for *C. albicans* (38), resistance to fluconazole often correlates with higher residual ergosterol levels after drug application. To investigate the possible role of ergosterol in mediating the effect of *MGE1* overexpression on fluconazole susceptibility, we measured ergosterol in the overexpression mutant. As can be seen from Fig. 2A, in the absence of fluconazole, there was only a small difference between the control and the strain overexpressing *MGE1*. Upon treatment with fluconazole, however, the fraction of ergosterol remaining in the mutant was significantly higher than the control (Fig. 2A and C). This phenotype was again independent of Pdr5, since the effect was still visible in the *pdr5*$\Delta$ mutant (Fig. 2B and C). To elucidate how *MGE1* overexpression affects sterol synthesis in general, we performed gas chromatography-mass spectrometry (GC-MS) analysis of the sterols isolated from our strains, in the absence and presence of fluconazole (Fig. S2A and B). As fluconazole targets Erg11, lanosterol accumulates and ergosterol levels decrease in the presence of the drug. Under these conditions,

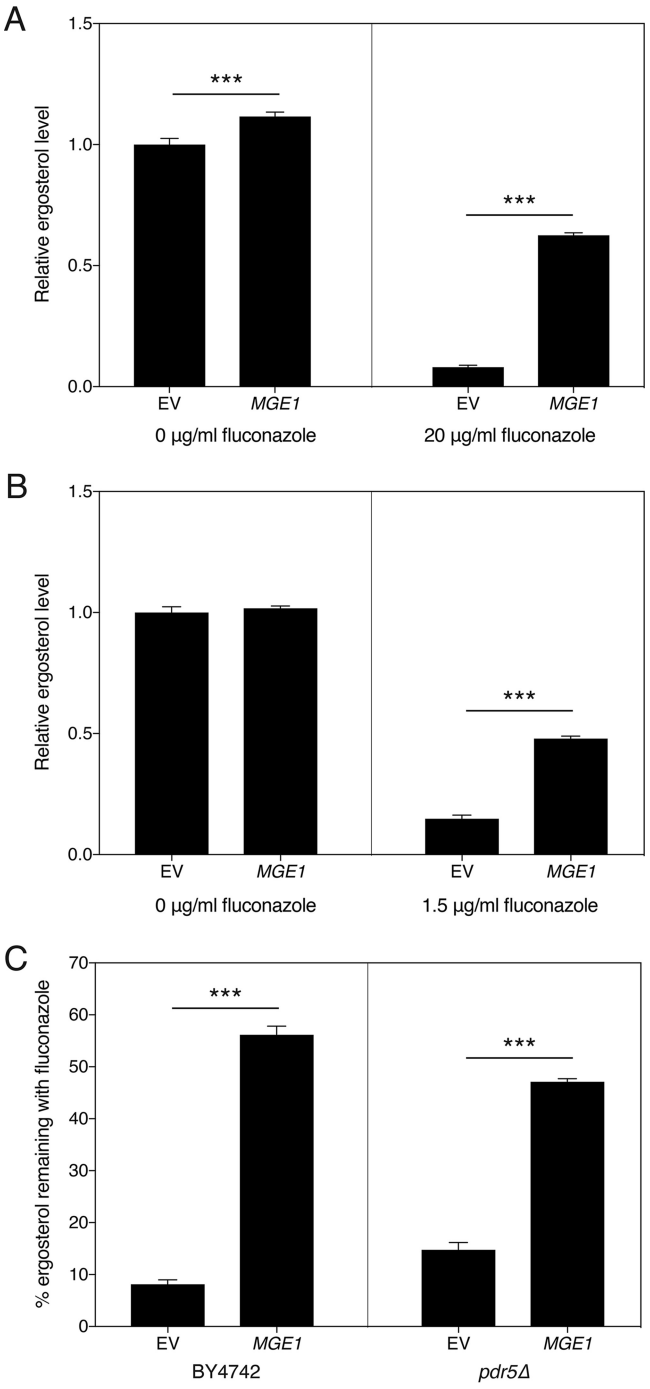


**FIG 2** Ergosterol levels are less affected by fluconazole when *MGE1* is overexpressed. *S. cerevisiae* cells were grown in SDglu medium for 24 h, in the presence or absence of fluconazole. (A and B) Ergosterol levels for transformants in the BY4742 background (A) and *pdr5*Δ background (B) are displayed. We note that for the *pdr5*Δ strain, a smaller amount of fluconazole had to be used, due to the increased sensitivity to the drug. The values were calculated relative to the average of the values from the untreated samples. For panels A and B, the interaction between both parameters was statistically significant ($P < 0.001$). (C) Percentage of residual ergosterol for both backgrounds, after fluconazole treatment. Statistical analysis was conducted by two-way ANOVA with Bonferroni correction (A and B) and an unpaired Student's *t* test (C); ***, $P < 0.001$.

lanosterol is also converted to 14-methylfecosterol and ultimately to the toxic compound 14-methylergosta-8,24(28)-dien-3$\beta$,6$\alpha$-diol, which represents an important aspect of the mode of action of the drug (39, 40). Interestingly, we saw that, compared to the control strain, overexpression of *MGE1* reduced the metabolic flux that leads to

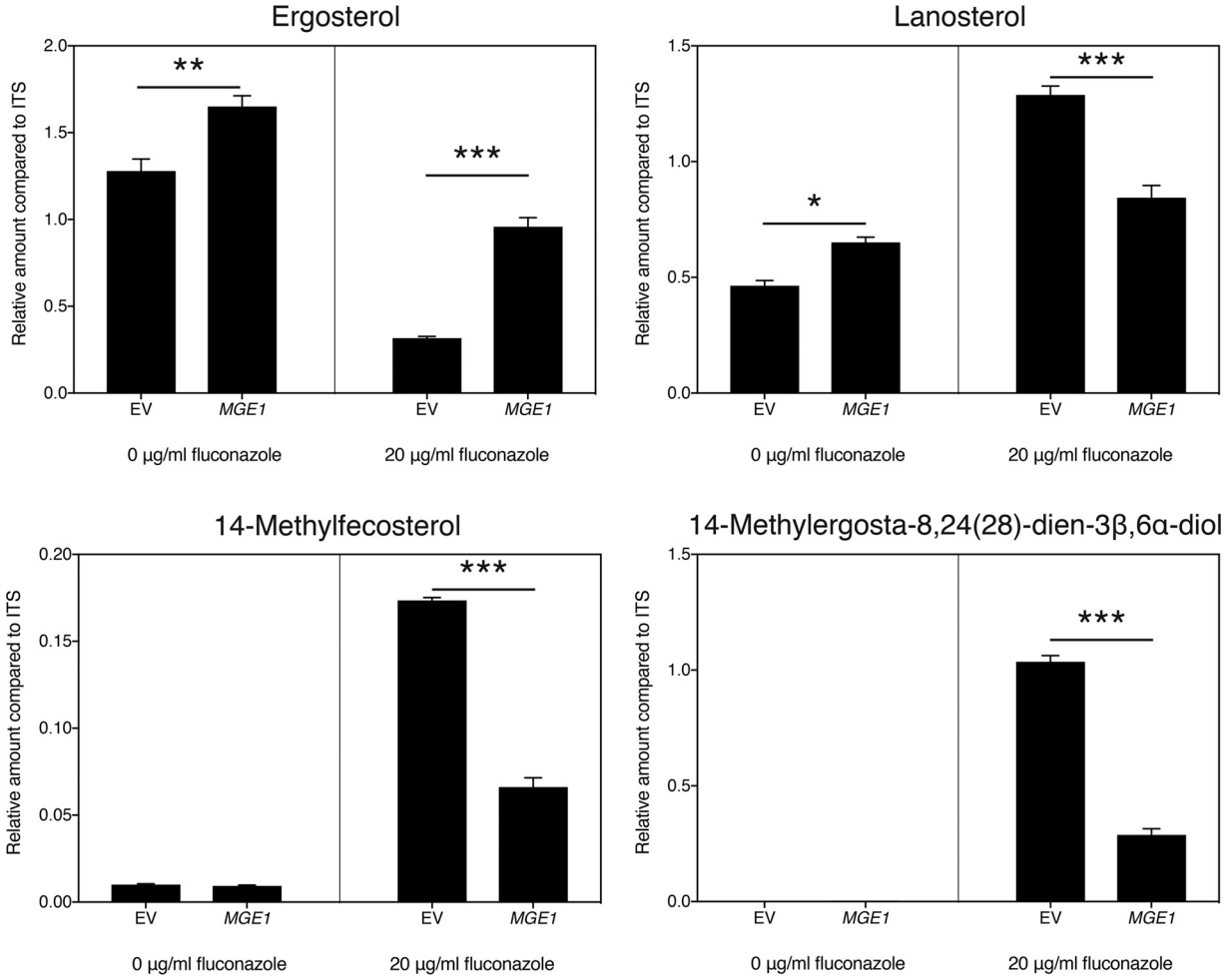


**FIG 3** *MGE1* overexpression alters the level of several sterols. Cells were grown in SDglu medium for 24 h in the presence or absence of fluconazole. Sterol levels were determined by GC-MS and are displayed for ergosterol, lanosterol, 14-methylfecosterol, and 14-methylergosta-8,24(28)-dien-3$\beta$,6$\alpha$-diol. The values were calculated relative to the internal standard (ITS; cholestane). The interaction between the two parameters was significant for each sterol ($P < 0.05$). Statistical analysis was conducted by two-way ANOVA with Bonferroni correction; *, $P < 0.05$; **, $P < 0.01$; ***, $P < 0.001$. Data from other sterols that were detected, but that were generally less abundant or could not be identified, are displayed in Fig. S2A.

toxic sterol formation, thereby maintaining a higher flux toward ergosterol production (Fig. 3).

As Erg11 is the target of fluconazole and the point in the sterol synthesis pathway where progress to either ergosterol or the toxic sterol is defined, it seems valid to hypothesize that Erg11 might be the enzyme linking Mge1 to ergosterol. We checked the expression levels and protein levels of *ERG11* and the Erg11 protein, respectively, in the mutant and control strains in both the absence and presence of fluconazole. Remarkably, gene expression levels and protein levels remained the same and were reduced, respectively, rather than upregulated in the *MGE1* overexpression strain (Fig. S3A and B). For the Western blot analysis, we used an anti-hemagglutinin (anti-HA) antibody and the AFc202 strain, where *ERG11* was tagged chromosomally with a 3× HA tag, thus representing native expression. We verified that the $MIC_{flu}$ of this mutant is similar to that of the BY4742 wild-type strain, as can be seen in Table S4. Apart from *ERG11*, other genes encoding ergosterol biosynthesis enzymes have also been shown to be induced upon azole treatment (41–44). Still, we found that overexpression of *MGE1* did not significantly upregulate the expression of *ERG2*, *ERG3*, *ERG4*, *ERG5*, *ERG6*, *ERG7*, *ERG8*, *ERG9*, *ERG12*, *ERG19*, *ERG24*, or *ERG25* under either control or fluconazole-treated conditions (Fig. S3A). As described by MacPherson et al. in 2005 for *C. albicans*

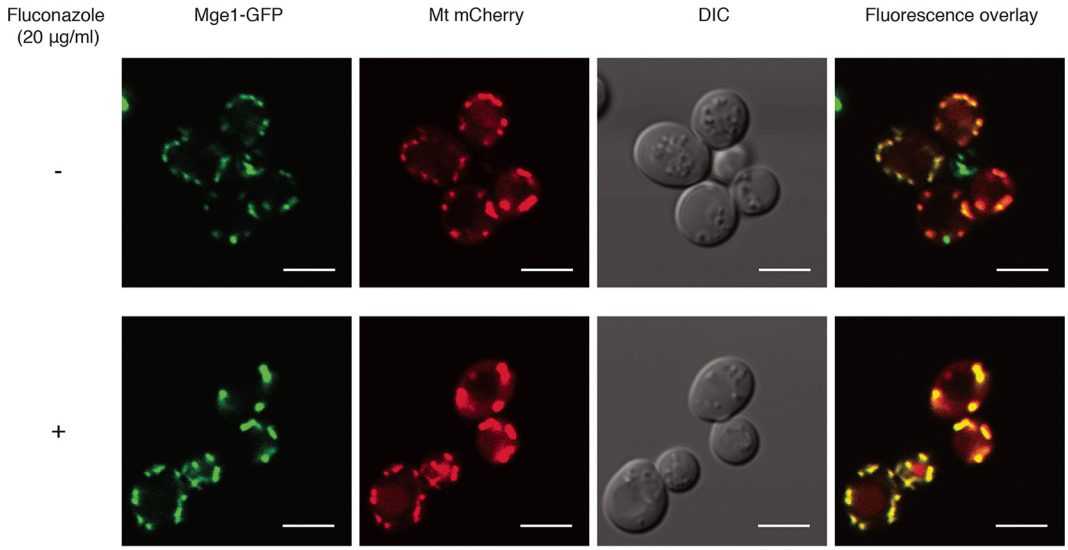


**FIG 4** Mge1 localizes to the mitochondria. The BY4742 strain expressing both *MGE1-GFP* and mitochondrially targeted (Mt) *mCherry* was incubated for 24 h in the absence or presence of 20 $\mu$g/ml fluconazole, pictures were taken afterward. The scale bar represents 5 $\mu$m. DIC, differential interference contrast.

(43), Upc2 confers resistance to antifungals by modulating expression of certain genes involved in ergosterol biosynthesis. We confirm here that Mge1 did not function upstream of Upc2 in increasing the $MIC_{flu}$, since *MGE1* overexpression still caused a decrease in fluconazole susceptibility in an *upc2*Δ strain (Table 1; Fig. S1C). Additionally, Upc2 did not influence *MGE1* expression, as can be seen from Fig. S3C. In summary, although Mge1 alters the flux through the sterol synthesis pathway, thereby maintaining increased ergosterol levels and decreasing toxic sterol levels, this does not appear to be mediated by changing the expression level of the fluconazole-dependent genes encoding the main biosynthesis enzymes in this sterol pathway.

**The Mge1-dependent decrease in fluconazole susceptibility requires the mitochondrial chaperone Ssq1.** Both known processes involving Mge1, i.e., Fe-S cluster formation and protein import across the inner mitochondrial membrane, are localized to the mitochondria. Although the literature also reports on the localization of Mge1 to this organelle (45), the experimental procedures used always consisted of *in vitro* rather than *in vivo* methods. To verify that Mge1 indeed functions inside the mitochondria, in the absence as well as the presence of fluconazole, we checked its localization by fluorescence microscopy. From Fig. 4, it can be seen that Mge1 localized to the mitochondria in the overexpression mutant, under both conditions. This indicates that the function by which Mge1 causes a decrease in the susceptibility to fluconazole must also be confined to this organelle. It was verified that *MGE1-GFP* overexpression still caused an increased $MIC_{flu}$ level (Table S4).

To further elucidate the mode of action by which Mge1 converts resistance to fluconazole, we postulated that this phenotype is effectuated by either of the downstream Hsp70 proteins. Ssc1 is part of the TIM23 complex spanning the inner mitochondrial membrane and works as an ATPase, providing energy to transport proteins into the mitochondria. A paralog of Ssc1, Ecm10, probably arose through genome duplication (82% amino acid identity) and is thought to have functions that overlap those of Ssc1 (46–48). It has been shown that Ecm10 also interacts with Mge1 (48). Ssq1 shows limited homology with Ssc1 (52% amino acid identity) and plays a role in one of the initial steps of Fe-S cluster formation, together with Mge1 (19). To determine whether the effect of *MGE1* overexpression on fluconazole susceptibility operates through Ssc1, Ecm10, or Ssq1, we verified if the resistance phenotype is still observed in mutants with a defect in either of the downstream pathways. Tom70 is part of the translocase of the outer mitochondrial membrane (TOM) complex, playing a role in

recognizing and importing mitochondrial proteins (49, 50). Deletion of the *TOM70* gene affects protein import into the mitochondria (50). The $MIC_{flu}$ of the *tom70*Δ strain was equal to that of the wild type (Fig. S1D; Table S4), and overexpression of *MGE1* in this strain resulted in an increase in the $MIC_{flu}$ similar to that seen with the wild type, indicating that full protein import into the mitochondria is not essential for the Mge1-related effect on fluconazole susceptibility (Fig. S1D; Table 1). As mentioned before, Ecm10 is a paralog of Ssc1. Since deletion of *ECM10*, in contrast to *SSC1*, is viable, we decided to see if overexpression of *MGE1* in this strain would still cause an increase in the $MIC_{flu}$. As can be seen from Fig. S1E and Table S4, the *ecm10*Δ strain had an $MIC_{flu}$ similar to that of the wild-type BY4742 strain. Overexpression of *MGE1* in this strain changed this $MIC_{flu}$ in the same way as was seen with BY4742 (Fig. S1E; Table 1), implying that Ecm10 is also not involved. Deletion of *SSQ1* is viable; therefore, we also tested the $MIC_{flu}$ of the *ssq1*Δ strain and found it to be significantly lower than that of the BY4742 wild-type strain (Fig. S1F; Table S4), in agreement with a previous report by Dagley et al. (51). Overexpression of *MGE1* in the *ssq1*Δ strain yielded remarkably few and slow-growing transformants (our unpublished observations), suggesting that combining a deletion of *SSQ1* with overexpression of *MGE1* alters the cells' fitness. Additionally, when *MGE1* was overexpressed, the $MIC_{flu}$ of the *ssq1*Δ strain did not increase compared to that of the empty vector control and even displayed a decrease (Fig. S1F; Table 1). This suggests that Ssq1 is necessary to establish the Mge1-mediated effect on fluconazole susceptibility.

**Activation of the iron regulon is necessary but not sufficient for Mge1 to exert its effect on fluconazole susceptibility.** It seems evident, from the literature and previous findings described above, that iron plays a role in regulating susceptibility to fluconazole (7, 27). In an attempt to clarify how this happens and how Mge1 provides a link in this process, we investigated the possible involvement of the iron regulon. Aft1 is a transcriptional regulator which induces transcription of genes involved in the recovery of iron upon iron starvation (22, 23). *AFT2* encodes a paralog of *AFT1*, which arose through gene duplication. The proteins encoded by the two genes have partially overlapping functions, with Aft2 being responsible for the iron metabolism when Aft1 is not present (24). Overexpression of *MGE1* still reduced the susceptibility to fluconazole in an *aft2*Δ strain, but this effect was lost in the *aft1*Δ strain (Fig. S1G; Table 1). As Aft1 is necessary for the Mge1-related effect, we speculated that, upon overexpression of the cochaperone gene, the expression of iron regulon genes might also be induced. We confirmed this for six iron regulon genes (Fig. 5). Next, we questioned whether mere activation of the iron regulon could explain the Mge1-regulated effect on fluconazole susceptibility or whether this is only part of the mechanism. Fra1 is a negative regulator of the iron regulon. In the presence of an as-yet-unknown signal coming from the Fe-S cluster metabolism in the mitochondria, Fra1 forms a complex with Fra2, Grx3, and Grx4 and inhibits the translocation of Aft1 to the nucleus, thereby inhibiting transcription of the iron regulon genes (52). Deletion of *FRA1* was shown to induce the iron regulon, even in the presence of large amounts of iron (52). We confirmed that deletion of *FRA1* induced expression of the iron regulon genes in our experimental setup as well. In Fig. 5, we show that the induction of expression in the *fra1*Δ strain was always similar to or higher than the induction seen upon *MGE1* expression, indicating the validity of the comparison. If activation of the iron regulon were the sole mechanism by which *MGE1* overexpression leads to fluconazole resistance, the *fra1*Δ strain should also show an increased $MIC_{flu}$ compared to that of the wild-type BY4742 strain. However, Table 1 and Fig. S1H show that this is not the case, indicating the requirement of yet another unknown process to work in conjunction with iron regulon activation in establishing fluconazole resistance downstream of Mge1. Thus, activation of the iron regulon is necessary but is insufficient by itself to induce resistance against fluconazole downstream of Mge1.

**Increased dosage of Mge1 also acts as a suppressor of susceptibility to fluconazole in *C. glabrata*.** *C. glabrata* and *C. albicans* are two of the most frequently isolated pathogenic fungi in humans (53). For the past few years, *C. glabrata* infections

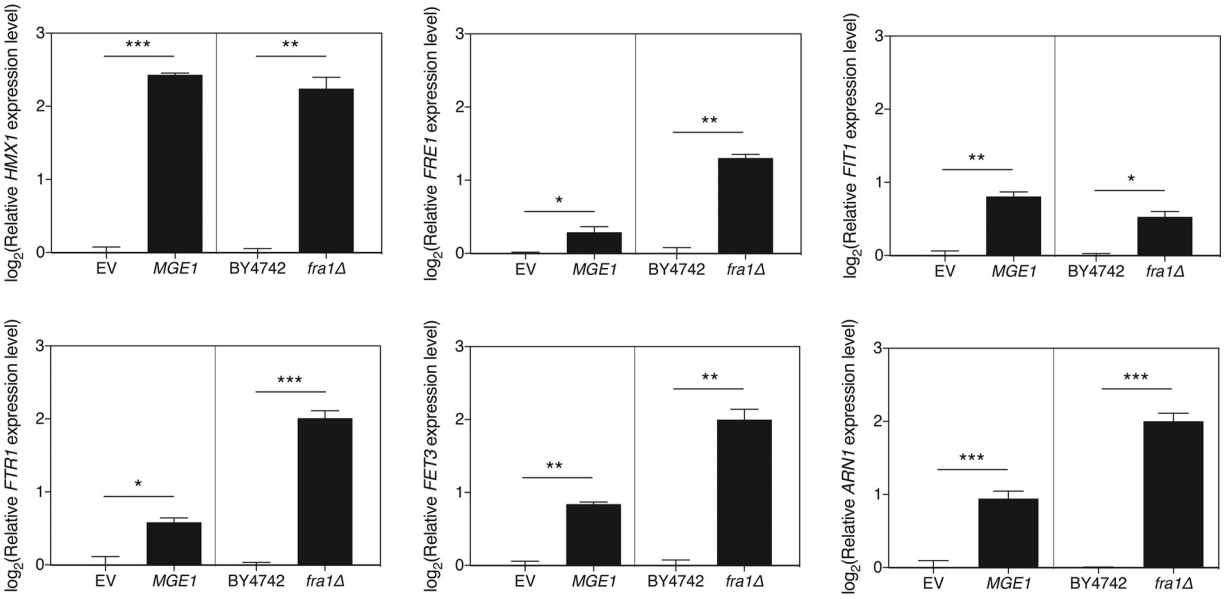


**FIG 5** Expression of typical iron regulon genes increases upon overexpression of *MGE1* or deletion of *FRA1*. Expression of the representative iron regulon genes *HMX1*, *FRE1*, *FIT1*, *FTR1*, *FET3*, and *ARN1* was analyzed by qRT-PCR. For each gene, the left panel shows the effect of overexpressing *MGE1* in the BY4742 strain versus the EV control. The right panel shows comparisons of the levels of gene expression between BY4742 and *fra1*Δ strains. Results are displayed as the average of $\log_2$(Y) transformed values with the SEM. The values were calculated relative to the averages of the values from the respective controls. Statistical analysis was conducted by unpaired Student's *t* test with Bonferroni correction; *, $P < 0.05$; **, $P < 0.01$; ***, $P < 0.001$.

have been on the rise in northern Europe and the United States, indicating a need for specific research and drug development (54). Its evolutionarily close relationship with *S. cerevisiae* (55) implies that the phenotype that we observed for *S. cerevisiae MGE1* (*ScMGE1*) overexpression with respect to susceptibility to fluconazole might also apply to *MGE1* in *C. glabrata*. The closest *C. glabrata* orthologue of *S. cerevisiae* Mge1 is encoded by CAGL0J03850g, which is indicated as an uncharacterized ORF in the Candida Genome Database (CGD) (56). Comparing the protein sequence of *S. cerevisiae* Mge1 to that of its orthologue in *C. glabrata* yielded an amino acid identity of 68%. We thus refer to the *C. glabrata* orthologue as *C. glabrata* Mge1 (*Cg*Mge1). To investigate the effect of *CgMGE1* overexpression on susceptibility to fluconazole, we created two plasmids expressing the *CgMGE1* ORF, together with its terminator, from either the *CgPGK1* promoter or the *CgTDH3* promoter. Overexpression of *MGE1* in the transformed 2001HTL strains was verified using qRT-PCR, yielding fold increases of 24.9 (SEM, 5.54) for the *CgPGK1* promoter and 42.9 (SEM, 4.0) for the *CgTDH3* promoter compared to the control. Both Etest and broth microdilution analyses indicated that overexpression of *CgMGE1* in *C. glabrata* also increased the $MIC_{flu}$ (Table 1; Fig. S4A). The microdilution assay was performed on RPMI medium containing 0.2% glucose, while the Etest analysis was performed on RPMI agar plates containing both 0.2% and 2% glucose. The addition of extra glucose generally enhances the ability to visually inspect the $MIC_{flu}$, as formerly shown for *C. albicans* (57). As with *S. cerevisiae*, no significant effect of *CgMGE1* overexpression on tolerance was observed (Fig. S4B). In summary, these data suggest that, similarly to the situation in *S. cerevisiae*, *Cg*Mge1 plays a role in regulating susceptibility to fluconazole in *C. glabrata*.

**Overexpression of *MGE1* affects both resistance and tolerance in *C. albicans*.** Although the incidence of *C. glabrata* infections is increasing steadily in certain parts of the world, *C. albicans* is still the most prevalent cause of *Candida* infections worldwide (53). The evolutionary distance between this important pathogen and *S. cerevisiae* is, however, bigger than is the case for *C. glabrata*, indicating that *S. cerevisiae* might not be as good a model system for *C. albicans* as it is for *C. glabrata* (55). To check whether Mge1 is also involved in fluconazole susceptibility in *C. albicans*, we generated a

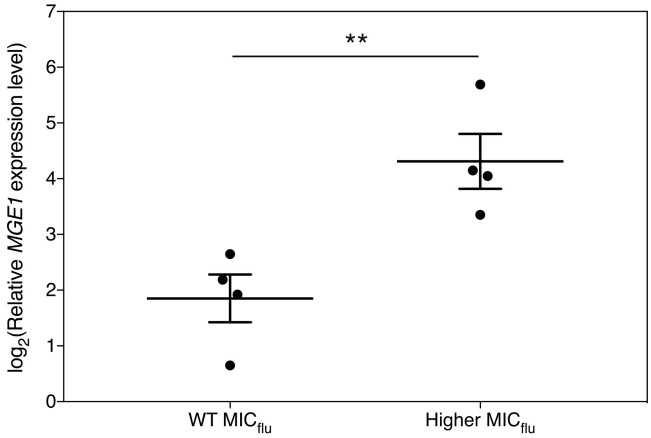


**FIG 6** Overexpression level of *CaMGE1* in SC5314 correlates with the $MIC_{flu}$. *C. albicans* strain SC5314 was transformed with plasmid pLDa01 (Clp10-*CaMGE1*), and fluconazole sensitivity was determined with the Etest method. Transformants with $MIC_{flu}$ values that were similar to or higher than those seen with the EV control strains were obtained. For 4 transformants of each group, *CaMGE1* expression was determined by qRT-PCR, and the values were calculated relative to the average of the values from the EV control samples (see Fig. S5). The results are displayed as the average of $\log_2$(y) transformed values with the SEM along with the separate data points. The statistical analysis was conducted by unpaired Student's *t* test; **, $P < 0.01$. WT, wild type.

plasmid where *C. albicans MGE1* (*CaMGE1*) is under the control of the strong, constitutive *CaACT1* promoter. The Clp10 plasmid integrates in the genome at the *RP10* locus, where it should stably overexpress *CaMGE1* (58). The SC5314 strain was transformed with either the overexpression construct or the empty plasmid as a control. While the control transformants displayed a uniform $MIC_{flu}$ phenotype, overexpression of *CaMGE1* yielded two phenotypes. One group of transformants did not show an alteration in the $MIC_{flu}$ compared to the EV controls, while others showed an increased $MIC_{flu}$ which was mainly visible after 24 h of incubation (Fig. S5A and B). We reasoned that this could have been due to different levels of overexpression of *CaMGE1*, as we also had observed various levels of (over)expression in the past upon transformation of *C. albicans* (our unpublished observations). It is speculated that this might be due to the high plasticity of the *C. albicans* genome (59). Here, we confirm a highly variable level of *CaMGE1* overexpression in our transformants and demonstrate that the observed variation is largely due to the various results with respect to copy number integration of the plasmid in the genome (Fig. S5A). As can be seen in Fig. 6, the highest *CaMGE1* expression levels of the transformants correlated with an increase in the $MIC_{flu}$, indicating that, above a certain threshold of *CaMGE1* expression, increased resistance to fluconazole was detected. Intriguingly, for those strains, we found a decrease in tolerance (Fig. S5C). Our results thus indicate that upon (sufficient) overexpression of *MGE1*, resistance of *C. albicans* to fluconazole is increased, similarly to the situation in *S. cerevisiae* and *C. glabrata*. In contrast to the latter organisms, however, this increased resistance in *C. albicans* seems to come at the cost of a lower tolerance to the same drug.

## DISCUSSION

In this study, we identified Mge1, a cochaperone involved in Fe-S cluster metabolism and protein import into the mitochondria, as a multicopy suppressor of fluconazole susceptibility (16, 17, 19). When an *S. cerevisiae* mutant strain grows in the presence of an otherwise inhibitory chemical, it is important to consider increased $rho^{0/-}$ formation and drug efflux as possible modes of action (60). Several groups have already reported on a relation between Mge1, or its downstream chaperones, and mtDNA stability (18, 30, 61, 62). However, we show here that neither loss of the mitochondrial DNA nor drug efflux through Pdr5 can solely account for the increased growth of the *MGE1* overexpression strain on fluconazole (33, 34).

The target of fluconazole is Erg11, an enzyme involved in the biosynthesis of ergosterol (5, 6). In this report, we show that ergosterol levels are elevated in an *S. cerevisiae* strain where *MGE1* is overexpressed, a phenomenon which is much more prominent after the addition of fluconazole. It thus seems that Mge1 evokes a protective mechanism by which the cell can retain higher levels of ergosterol upon treatment with fluconazole. A detailed analysis of the sterol spectra of our strains indicated that, upon fluconazole addition, *MGE1* overexpression reduces the metabolic flux toward potential toxic sterols, most notably 14-methylergosta-8,24(28)-dien-3$\beta$,6$\alpha$-diol (39, 40). The reduced accumulation of this sterol, together with the retention of more ergosterol upon fluconazole treatment, illustrates how Mge1 reduces susceptibility to the drug. As Erg11 functions at the cross-section between the pathways leading to either ergosterol production or toxic sterol accumulation, we analyzed the abundance of this enzyme but found no increase at the level of either gene expression or protein abundance upon *MGE1* overexpression. Analysis of the expression of other *ERG* genes, known to be regulated by fluconazole, could also not identify a transcriptional mechanism explaining the observed sterol profiles. It is possible that *MGE1* overexpression specifically alters the enzyme activity of Erg11 or of other ergosterol biosynthesis enzymes, rather than their expression. It remains unclear how Mge1, operating in the mitochondria, would impact ergosterol biosynthesis, which mainly takes place in the endoplasmic reticulum (ER) (63).

To further elucidate how Mge1 function might be linked to fluconazole susceptibility, we looked at the known Mge1 effectors. We demonstrated the involvement of the Hsp70 chaperone Ssq1, as this chaperone is necessary for the cell to retain its $MIC_{flu}$ at the wild-type level and as overexpression of *MGE1* in the *ssq1*$\Delta$ strain could not increase fluconazole resistance. Ssq1 is essential for mitochondrial Fe-S cluster metabolism, which somehow functions as an iron-sensing system in the cell, since in the presence of sufficient iron, an inhibitory signal originates from this metabolism and impairs transcription of the iron regulon genes (64). Intriguingly, we found that overexpressing *MGE1* in the wild-type strain causes a significant increase in expression of characteristic iron regulon genes. Furthermore, deleting *AFT1*, the gene encoding the main transcriptional regulator of the iron regulon, impairs the effect of Mge1 on fluconazole susceptibility, indicating the strict dependence of our phenotype on this regulon. It is possible that overloading the cell with Mge1 might impair, rather than increase, the cochaperone's function. This would then lead to a reduced Fe-S signal, thereby activating the iron regulon and generating fluconazole resistance by modulating sterol synthesis, as shown before under iron-limiting conditions in yeast (65, 66). Several elements argue against such a straightforward mechanism, however. First of all, Schmidt et al. reported that overexpression of *MGE1* increases the activity of Ssq1 (67), implying increased rather than impaired Fe-S cluster biogenesis. Second, impairing Ssq1 function does not lead to fluconazole resistance, as we observed that the *ssq1*$\Delta$ strain was more sensitive, and not resistant, to fluconazole. Finally, although we demonstrate the dependency of fluconazole resistance on the activation of the iron regulon, we also clearly show that this is not sufficient, since mere activation of the iron regulon through *FRA1* deletion does not cause any change in the $MIC_{flu}$. It thus remains to be investigated how Mge1 activity is linked to the iron regulon on one side and to fluconazole susceptibility on the other side. It is tempting to speculate that increasing Mge1 activity alters the balance in Fe-S cluster proteins in a specific way, causing fluconazole resistance via two separate pathways: by activating the iron regulon and simultaneously by some other, yet-to-be-elucidated mechanism. Future in-depth analysis of the changes in the Fe-S cluster metabolism upon *MGE1* overexpression would thus represent a valuable system to elucidate this mechanism. This analysis could pinpoint Fe-S species which regulate the resistance to fluconazole through modulation of ergosterol metabolism, i.e., by reducing toxic sterol production and increasing ergosterol retention. At the same time, as the identities of the specific Fe-S species which are involved in regulating the iron regulon are still unknown at present, such an analysis would also provide crucial information on this topic.

Apart from the observations made in *S. cerevisiae*, we also validated the Mge1-related effect on fluconazole resistance in the fungal pathogens *C. glabrata* and *C. albicans*. Very little is known about Fe-S cluster metabolism in either pathogen. The *C. glabrata* orthologue of *ScSSQ1* is uncharacterized (56). The *C. albicans* orthologue was characterized recently (68); these researchers confirmed a role for *Ca*Ssq1 in iron metabolism and iron regulon modulation. More research is necessary to uncover the exact role of the Mge1-Ssq1 module in regulating the susceptibility of fungal cells to fluconazole. Knowledge of this mechanism could provide novel drug targets which would increase the antifungal potential of azoles in combinatorial therapies.

## MATERIALS AND METHODS

**Strains and plasmids.** All *S. cerevisiae* strains used in this study are isogenic with respect to the BY4742 laboratory strain and are listed in Table S1 in the supplemental material. Strain AFc202, carrying a chromosomal 3×HA C-terminal tag at *ERG11*, was constructed by transforming BY4742 with a PCR fragment obtained using primers listed in Table S2 and plasmid pMPY-3xHA as a template (69). Transformants were allowed to pop out the *URA3* marker by homologous recombination, and uracil auxotrophs were selected using 5-fluoroorotic acid (5-FOA). The BY4742 strain was made rho$^0$ by repeated growth in the presence of 25 $\mu$g/ml ethidium bromide in minimal medium, as described in reference 70. Deletion of *PDR5* in BY4742 and rho$^0$ strains was accomplished by amplification of the hygromycin resistance marker gene from plasmid pFA6a-*hphNT1* (71) and consequent transformation. *C. glabrata* and *C. albicans* strains used in the experiments are also listed in Table S1. *C. albicans* strains LDa01 to LDa08 were generated by transforming the StuI-linearized pLDa01 plasmid in SC5314. The LDa09 strain was created similarly by integration of the empty Clp10-*NAT1* plasmid. All specific genotypes were checked by diagnostic PCR.

Plasmids are listed in Table S3. Plasmid pAFc86 contains *MGE1* under the control of its promoter and terminator. The SnaBI-XhoI fragment from the Lacroute library plasmid was cloned into YEplac195 linearized using SmaI. Plasmid pESc01 is similar to pAFc86, with fusion of *MGE1* to the gene encoding green fluorescent protein [GFP(S65T)]. This plasmid was created by amplification of the *MGE1* promoter, the *MGE1* ORF, the *GFP* gene, and the *MGE1* terminator and assembly of them in the YEPlac195 plasmid using In-Fusion cloning (Clontech). The mitochondria were marked by transforming a plasmid containing *mCherry* fused to a mitochondrial targeting sequence in the appropriate strains (72). Plasmids pESg01 and pESg02 were generated by assembling the *CgPGK1* promoter or *CgTDH3* promoter and the *CgMGE1* ORF and its terminator in the pCgACH backbone (73) by In-Fusion cloning. Plasmid Clp10-*NAT1* was generated by exchanging the *CaURA3* marker together with its promoter and terminator from the Clp10 plasmid (58) for the dominant *C. albicans* optimized *NAT1* gene together with a *CaACT1* promoter and terminator (74), using NotI and SpeI. Another *CaACT1* promoter and terminator were added in the multiple cloning site, opened with MluI-NheI and XhoI-KpnI, respectively. Plasmid pLDa01 was generated by integrating the *CaMGE1* gene in the PstI-ClaI-cut Clp10-*NAT1* vector.

**Growth conditions: media and chemicals.** *S. cerevisiae* strains were grown in SDglu, unless stated otherwise. This medium contains 0.17% Difco yeast nitrogen base without amino acids or ammonium sulfate, 0.5% ammonium sulfate, and 2% glucose. Liquid medium was pH adapted to pH 5.5. For solid medium, the pH was set at 6.5 and 1.6% agar was added. Depending on the strain, additional amino acids or nucleotides were added according to the method described in reference 75. For spot assays, fluconazole (F8929; Sigma) and doxycycline (D9891; Sigma) were added to the medium at concentrations of 10 or 20 $\mu$g/ml and 50 or 100 $\mu$g/ml, respectively. The procedure used to screen for multicopy suppressors of susceptibility to fluconazole-doxycycline was described in reference 7. For some specific experiments, YPD medium (containing 1% yeast extract, 2% peptone, and 2% glucose) was used. *C. albicans* and *C. glabrata* strains were pregrown in synthetic complete glucose (SCglu) medium or SC(-HIS)glu medium, composed of SDglu with the addition of complete or drop-out CSM (MP Biomedicals). Assays were carried out in filter-sterilized RPMI 1640 medium with L-glutamine (R6504; Sigma) and buffered with 0.165 M morpholinepropanesulfonic acid at pH 7. Depending on the assay, autoclave-sterilized and precooled agar and/or 1.8% glucose was added to the medium. Cell cultures containing fluconazole or doxycycline were always kept in the dark.

**Determination of fluconazole susceptibility: MIC$_{flu}$ evaluation, tolerance assays, and spot assays.** To determine the MIC$_{flu}$ for the strains, two methods were always used in parallel. In the Etest method (BioMérieux), the MIC$_{flu}$ was determined as the concentration of fluconazole where the halo of growth inhibition/retardation intersected with the strip. Overnight cultures were adjusted to an optical density at 600 nm (OD$_{600}$) of 0.5 in water for *S. cerevisiae* and an OD$_{600}$ of 0.2 for *C. glabrata* and *C. albicans* and were spread on SDglu or RPMI (with 0.2% or 2% glucose) plates. The strips were placed onto the lawn of cells, and the plates were incubated at 30°C or 37°C for 48 h. Broth microdilution assays were conducted according to the Clinical Laboratory and Standards Institute (CLSI) standard methods (76). Round-bottom, UV-sterilized 96-well microtiter plates were used, where all wells were filled with 0.5 to 2.5 × 10$^3$ cells/ml, 0 to 128 $\mu$g/ml fluconazole in 1/2 dilutions, and SDglu or RPMI medium (the latter with 0.2% glucose). For *C. albicans*, the fluconazole dilution series was set between 0 and 32 $\mu$g/ml fluconazole. After incubation of the plates at 30°C or 37°C under nonshaking conditions for 48 h, we measured the OD$_{600}$ of the resuspended cultures in each well to obtain quantitative and objective data. A dose-response curve was created, and the MIC values were calculated by subtracting the background OD values determined for the medium from all measured data points and subsequent normalization to

the condition without fluconazole. The concentrations of the drug, between which the relative OD falls below 50 or 10% of the no-drug OD are called the $MIC_{50}$ and the $MIC_{90}$, respectively. To evaluate the drug tolerance of our strains, we generated dose-response curves based on CFU counts for the *MGE1* overexpression strain and empty vector control. The wells of the broth microdilution assay plate were resuspended, and each culture was diluted and plated. The drug tolerance was determined by checking the CFU counts under the conditions seen with the two highest fluconazole concentrations. For spot assays, overnight cultures were adapted to an $OD_{600}$ of 1, and 5 serial 1/5 dilutions were spotted. SDglu medium was used with different concentrations of fluconazole and doxycycline. The plates were incubated at 30°C for 48 or 72 h. All experiments were conducted with at least three biological repeats, and representative results are shown.

**Sterol measurement.** Sterols were extracted according to the method described in reference 77, with a few adaptations. In summary, cells were grown for 24 h in minimal medium, with or without 20 $\mu$g/ml fluconazole. The cells were collected, resuspended in saponification medium, and subjected to vortex mixing. The samples were incubated for 1 h at 80°C, after which 1 ml of water and 4 ml of hexane were added. After mixing, the two layers were allowed to separate. For spectrophotometrical analysis, UV-transmittable 96-well microtiter plates (3635; Costar Corning) were used to allow measurement of the $OD_{281}$ and $OD_{230}$. A formula from reference 38 was used to measure the percentages of ergosterol (corrected for cellular wet weight and resuspension volume). For GC-MS analysis, the sterols were extracted twice with hexane, which was then evaporated by vacuum centrifugation. The sterols were resuspended in 100 $\mu$l silylating mixture (85432; Sigma) and incubated at room temperature for 30 min. Finally, 500 $\mu$l hexane was added and the samples were immediately stored at −20°C for later analysis by GC-MS. One microliter of the sample was injected into a gas chromatograph-mass spectrometer (Shimadzu QP2010 Ultra Plus) equipped with an HP-5ms nonpolar column (Agilent) (30 m in length, 0.25-mm inner diameter [id.]; 0.25-$\mu$m thin layer). Helium was used as carrier gas with a flow rate of 1.4 ml/min. Injection was carried out at 250°C in split mode after 1 min and with a ratio of 1:10. The temperature was first held at 50°C for 1 min and then allowed to rise to 260°C at a rate of 50°C/min, followed by a second ramp of 2°C/min until 325°C was reached; that temperature was maintained for 3 min. The mass detector was operated in scan mode (50 to 600 atomic mass units [amu]), using electron impact ionization (70 eV). The temperatures of the interface and detector were 290°C and 250°C, respectively. A mix of linear *n*-alkanes (from $C_8$ to $C_{40}$) was injected to serve as external retention index markers. Sterols were identified by their retention time relative to the internal standard (cholestane) and specific mass spectrometric patterns using AMDIS version 2.71. The deconvoluted spectra were matched to GC-MS libraries described in reference 78 and NIST/EPA/NIH version 2011. Analysis was performed by integration over the base ion of each sterol, and abundance was calculated relative to the internal standard, comparing the relative peak areas of the compounds across treatments using two-way ANOVA with Bonferroni correction. Apart from the *P* values for pairwise comparison, the *P* values for interaction between the two parameters are also described.

**RNA extraction and gene expression analysis by qRT-PCR.** *S. cerevisiae* strains were grown in SDglu medium at 30°C for 24 h, with or without 20 $\mu$g/ml fluconazole. *C. glabrata* and *C. albicans* cells were incubated for 8 h at 37°C or 30°C in RPMI medium, with or without 1 $\mu$g/ml fluconazole. Cells were washed with ice-cold water, resuspended in TRIzol (Thermo, Fisher), and broken using glass beads and a FastPrep machine (MP Biomedicals). RNA was extracted by respective addition of chloroform and isopropanol and washed three times with 70% ethanol. Equal amounts of RNA were treated with a DNase enzyme (New England Biolabs) and converted to cDNA (iScript cDNA synthesis kit; Bio-Rad). Real-time quantitative PCR (qPCR) reactions were conducted using GoTaq polymerase (Promega) and a StepOnePlus real-time PCR device (Thermo, Fisher). Data were analyzed using qBasePlus software (Biogazelle) (79). Further data analysis and statistics analysis of $\log_2(Y)$ transformed expression values were performed with Graphpad Prism. Transformation of the data points was performed to enable the use of standard statistical methods. Graphs show the means of the transformed values, together with their SEM. The statistical method used is mentioned under each figure. Copy number analysis of the genomic DNA of transformants was performed by qPCR, as described above.

**Western blotting.** *S. cerevisiae* strains were grown in SDglu medium for 24 h at 30°C, with or without 20 $\mu$g/ml fluconazole. Cells were washed with lysis buffer (200 mM sorbitol, 20 mM HEPES–KOH [pH 6.8], 1 mM EDTA, 50 mM potassium acetate and protease inhibitors [Roche]), and glass beads were added to break them using a FastPrep machine. The amount of proteins was quantified using the Pierce protein assay (Thermo, Fisher), and 6 $\mu$g was loaded per well on an Invitrogen NuPage Novex bis-Tris gradient gel (4% to 12%). We used anti-HA (12013819001; Roche) and anti-Pgk1 (459250; Invitrogen) as loading controls. The blots were visualized using a FujiFilm LAS-4000 mini system and accompanying software.

**Fluorescence microscopy.** To determine the location of Mge1-GFP inside the cell, we used a FluoView FV1000 confocal microscope (Olympus IX81) and its software. We visualized GFP with a 488-nm argon laser and BA505-540 emission filter and mCherry with a 559-nm laser and BA575-675 emission filter. A 60× UPlanSApo (numerical aperture [NA], 1.35) objective lens was used.

## SUPPLEMENTAL MATERIAL

Supplemental material for this article may be found at https://doi.org/10.1128/mBio.00201-17.

**FIG S1,** PDF file, 8 MB.

**FIG S2,** PDF file, 0.8 MB.

**FIG S3,** PDF file, 0.3 MB.

**FIG S4,** PDF file, 1.6 MB.
**FIG S5,** PDF file, 1.4 MB.
**TABLE S1,** PDF file, 0.1 MB.
**TABLE S2,** PDF file, 0.1 MB.
**TABLE S3,** PDF file, 0.1 MB.
**TABLE S4,** PDF file, 0.1 MB.

## ACKNOWLEDGMENTS

We thank Cindy Colombo and Ilse Palmans for technical assistance and Nico Vangoethem for great help with the figures. We thank Hélène Tournu for making the CIp10-*NAT1* plasmid. L.D., E.S., A.F., and B.H.-M. designed and executed all experiments. All of us were involved in discussion of the results and revision of the manuscript.

L.D. and E.S. were supported personally by the FWO (Fund for Scientific Research Flanders). We further acknowledge financial project support from the FWO (G.OD48.13), the Research Fund of KU Leuven (GOA/13/006), and the Interuniversity Attraction Poles Programme initiated by the Belgian Science Policy Office (IAP P7/28). Research in the laboratory of K.V. is supported by VIB, AB-InBev-Baillet Latour Fund, FWO, VLAIO, European Research Council (ERC) Consolidator grant CoG682009, and Human Frontier Science Program (HFSP) grant 246 RGP0050/2013.

## REFERENCES

1. Brown GD, Denning DW, Gow NA, Levitz SM, Netea MG, White TC. 2012. Hidden killers: human fungal infections. Sci Transl Med 4:165rv13. https://doi.org/10.1126/scitranslmed.3004404.
2. Ostrosky-Zeichner L, Casadevall A, Galgiani JN, Odds FC, Rex JH. 2010. An insight into the antifungal pipeline: selected new molecules and beyond. Nat Rev Drug Discov 9:719–727. https://doi.org/10.1038/nrd3074.
3. Roemer T, Krysan DJ. 2014. Antifungal drug development: challenges, unmet clinical needs, and new approaches. Cold Spring Harb Perspect Med 4:e019703. https://doi.org/10.1101/cshperspect.a019703.
4. Shapiro RS, Robbins N, Cowen LE. 2011. Regulatory circuitry governing fungal development, drug resistance, and disease. Microbiol Mol Biol Rev 75:213–267. https://doi.org/10.1128/MMBR.00045-10.
5. Vanden Bossche H. 1985. Biochemical targets for antifungal azole derivatives: hypothesis on the mode of action. Curr Top Med Mycol 1:313–351. https://doi.org/10.1007/978-1-4613-9547-8_12.
6. Kelly SL, Arnoldi A, Kelly DE. 1993. Molecular genetic analysis of azole antifungal mode of action. Biochem Soc Trans 21:1034–1038. https://doi.org/10.1042/bst0211034.
7. Fiori A, Van Dijck P. 2012. Potent synergistic effect of doxycycline with fluconazole against *Candida albicans* is mediated by interference with iron homeostasis. Antimicrob Agents Chemother 56:3785–3796. https://doi.org/10.1128/AAC.06017-11.
8. Delarze E, Sanglard D. 2015. Defining the frontiers between antifungal resistance, tolerance and the concept of persistence. Drug Resist Updat 23:12–19. https://doi.org/10.1016/j.drup.2015.10.001.
9. Laloraya S, Gambill BD, Craig EA. 1994. A role for a eukaryotic GrpE-related protein, Mge1p, in protein translocation. Proc Natl Acad Sci U S A 91:6481–6485. https://doi.org/10.1073/pnas.91.14.6481.
10. Verghese J, Abrams J, Wang Y, Morano KA. 2012. Biology of the heat shock response and protein chaperones: budding yeast (*Saccharomyces cerevisiae*) as a model system. Microbiol Mol Biol Rev 76:115–158. https://doi.org/10.1128/MMBR.05018-11.
11. Hartl FU, Hayer-Hartl M. 2009. Converging concepts of protein folding *in vitro* and *in vivo*. Nat Struct Mol Biol 16:574–581. https://doi.org/10.1038/nsmb.1591.
12. Mayer MP, Bukau B. 2005. Hsp70 chaperones: cellular functions and molecular mechanism. Cell Mol Life Sci 62:670–684. https://doi.org/10.1007/s00018-004-4464-6.
13. Bolliger L, Deloche O, Glick BS, Georgopoulos C, Jenö P, Kronidou N, Horst M, Morishima N, Schatz G. 1994. A mitochondrial homolog of bacterial GrpE interacts with mitochondrial hsp70 and is essential for viability. EMBO J 13:1998–2006.
14. Laloraya S, Dekker PJ, Voos W, Craig EA, Pfanner N. 1995. Mitochondrial GrpE modulates the function of matrix Hsp70 in translocation and maturation of preproteins. Mol Cell Biol 15:7098–7105. https://doi.org/10.1128/MCB.15.12.7098.
15. Neupert W, Herrmann JM. 2007. Translocation of proteins into mitochondria. Annu Rev Biochem 76:723–749. https://doi.org/10.1146/annurev.biochem.76.052705.163409.
16. Miao B, Davis JE, Craig EA. 1997. Mge1 functions as a nucleotide release factor for Ssc1, a mitochondrial Hsp70 of *Saccharomyces cerevisiae*. J Mol Biol 265:541–552. https://doi.org/10.1006/jmbi.1996.0762.
17. Craig EA, Kramer J, Kosic-Smithers J. 1987. SSC1, a member of the 70-kDa heat shock protein multigene family of *Saccharomyces cerevisiae*, is essential for growth. Proc Natl Acad Sci U S A 84:4156–4160. https://doi.org/10.1073/pnas.84.12.4156.
18. Ikeda E, Yoshida S, Mitsuzawa H, Uno I, Toh-e A. 1994 YGE1 is a yeast homologue of Escherichia coli grpE and is required for maintenance of mitochondrial functions. FEBS Lett 339:265–268. https://doi.org/10.1016/0014-5793(94)80428-1.
19. Strain J, Lorenz CR, Bode J, Garland S, Smolen GA, Ta DT, Vickery LE, Culotta VC. 1998. Suppressors of superoxide dismutase (*SOD1*) deficiency in *Saccharomyces cerevisiae*. Identification of proteins predicted to mediate iron-sulfur cluster assembly. J Biol Chem 273:31138–31144. https://doi.org/10.1074/jbc.273.47.31138.
20. Lill R, Hoffmann B, Molik S, Pierik AJ, Rietzschel N, Stehling O, Uzarska MA, Webert H, Wilbrecht C, Mühlenhoff U. 2012. The role of mitochondria in cellular iron-sulfur protein biogenesis and iron metabolism. Biochim Biophys Acta 1823:1491–1508. https://doi.org/10.1016/j.bbamcr.2012.05.009.
21. Lill R. 2009. Function and biogenesis of iron-sulphur proteins. Nature 460:831–838. https://doi.org/10.1038/nature08301.
22. Yamaguchi-Iwai Y, Dancis A, Klausner RD. 1995. *AFT1*: a mediator of iron regulated transcriptional control in *Saccharomyces cerevisiae*. EMBO J 14:1231–1239.
23. Yamaguchi-Iwai Y, Stearman R, Dancis A, Klausner RD. 1996. Iron-regulated DNA binding by the AFT1 protein controls the iron regulon in yeast. EMBO J 15:3377–3384.
24. Blaiseau PL, Lesuisse E, Camadro JM. 2001. Aft2p, a novel iron-regulated transcription activator that modulates, with Aft1p, intracellular iron use and resistance to oxidative stress in yeast. J Biol Chem 276:34221–34226. https://doi.org/10.1074/jbc.M104987200.
25. Mühlenhoff U, Gerber J, Richhardt N, Lill R. 2003. Components involved in assembly and dislocation of iron-sulfur clusters on the scaffold protein Isu1p. EMBO J 22:4815–4825. https://doi.org/10.1093/emboj/cdg446.
26. Schilke B, Forster J, Davis J, James P, Walter W, Laloraya S, Johnson J, Miao B, Craig E. 1996. The cold sensitivity of a mutant of *Saccharomyces cerevisiae* lacking a mitochondrial heat shock protein 70 is suppressed

by loss of mitochondrial DNA. J Cell Biol 134:603–613. https://doi.org/10.1083/jcb.134.3.603.
27. Prasad T, Chandra A, Mukhopadhyay CK, Prasad R. 2006. Unexpected link between iron and drug resistance of *Candida* spp.: iron depletion enhances membrane fluidity and drug diffusion, leading to drug-susceptible cells. Antimicrob Agents Chemother 50:3597–3606. https://doi.org/10.1128/AAC.00653-06.
28. Stettler S, Chiannilkulchai N, Hermann-Le Denmat S, Lalo D, Lacroute F, Sentenac A, Thuriaux P. 1993. A general suppressor of RNA polymerase I, II and III mutations in *Saccharomyces cerevisiae*. Mol Gen Genet 239:169–176.
29. Dujon B. 1981. Mitochondrial genetics and functions. Cold Spring Harb Monogr Arch 11:505–635. https://cshmonographs.org/index.php/monographs/article/viewArticle/4239.
30. Contamine V, Picard M. 2000. Maintenance and integrity of the mitochondrial genome: a plethora of nuclear genes in the budding yeast. Microbiol Mol Biol Rev 64:281–315. https://doi.org/10.1128/MMBR.64.2.281-315.2000.
31. Traven A, Wong JM, Xu D, Sopta M, Ingles CJ. 2001. Interorganellar communication. Altered nuclear gene expression profiles in a yeast mitochondrial dna mutant. J Biol Chem 276:4020–4027. https://doi.org/10.1074/jbc.M006807200.
32. Chen XJ, Clark-Walker GD. 1999. The petite mutation in yeasts: 50 years on. Int Rev Cytol 194:197–238. https://doi.org/10.1016/S0074-7696(08)62397-9.
33. Dunn CD, Lee MS, Spencer FA, Jensen RE. 2006. A genomewide screen for petite-negative yeast strains yields a new subunit of the i-AAA protease complex. Mol Biol Cell 17:213–226. https://doi.org/10.1091/mbc.E05-06-0585.
34. Dunn CD, Jensen RE. 2003. Suppression of a defect in mitochondrial protein import identifies cytosolic proteins required for viability of yeast cells lacking mitochondrial DNA. Genetics 165:35–45.
35. White TC. 1997. Increased mRNA levels of *ERG16*, *CDR*, and *MDR1* correlate with increases in azole resistance in *Candida albicans* isolates from a patient infected with human immunodeficiency virus. Antimicrob Agents Chemother 41:1482–1487.
36. Goldman GH, da Silva Ferreira ME, dos Reis Marques E, Savoldi M, Perlin D, Park S, Godoy Martinez PC, Goldman MH, Colombo AL. 2004. Evaluation of fluconazole resistance mechanisms in *Candida albicans* clinical isolates from HIV-infected patients in Brazil. Diagn Microbiol Infect Dis 50:25–32. https://doi.org/10.1016/j.diagmicrobio.2004.04.009.
37. Perea S, López-Ribot JL, Wickes BL, Kirkpatrick WR, Dib OP, Bachmann SP, Keller SM, Martinez M, Patterson TF. 2002. Molecular mechanisms of fluconazole resistance in *Candida dubliniensis* isolates from human immunodeficiency virus-infected patients with oropharyngeal candidiasis. Antimicrob Agents Chemother 46:1695–1703. https://doi.org/10.1128/AAC.46.6.1695-1703.2002.
38. Arthington-Skaggs BA, Jradi H, Desai T, Morrison CJ. 1999. Quantitation of ergosterol content: novel method for determination of fluconazole susceptibility of *Candida albicans*. J Clin Microbiol 37:3332–3337.
39. Watson PF, Rose ME, Ellis SW, England H, Kelly SL. 1989. Defective sterol C5-6 desaturation and azole resistance: a new hypothesis for the mode of action of azole antifungals. Biochem Biophys Res Commun 164:1170–1175. https://doi.org/10.1016/0006-291X(89)91792-0.
40. Kelly SL, Lamb DC, Corran AJ, Baldwin BC, Kelly DE. 1995. Mode of action and resistance to azole antifungals associated with the formation of 14 alpha-methylergosta-8,24(28)-dien-3 beta,6 alpha-diol. Biochem Biophys Res Commun 207:910–915. https://doi.org/10.1006/bbrc.1995.1272.
41. Bammert GF, Fostel JM. 2000. Genome-wide expression patterns in *Saccharomyces cerevisiae*: comparison of drug treatments and genetic alterations affecting biosynthesis of ergosterol. Antimicrob Agents Chemother 44:1255–1265. https://doi.org/10.1128/AAC.44.5.1255-1265.2000.
42. De Backer MD, Ilyina T, Ma XJ, Vandoninck S, Luyten WH, Vanden Bossche H. 2001. Genomic profiling of the response of *Candida albicans* to itraconazole treatment using a DNA microarray. Antimicrob Agents Chemother 45:1660–1670. https://doi.org/10.1128/AAC.45.6.1660-1670.2001.
43. MacPherson S, Akache B, Weber S, De Deken X, Raymond M, Turcotte B. 2005. *Candida albicans* zinc cluster protein Upc2p confers resistance to antifungal drugs and is an activator of ergosterol biosynthetic genes. Antimicrob Agents Chemother 49:1745–1752. https://doi.org/10.1128/AAC.49.5.1745-1752.2005.
44. Dimster-Denk D, Rine J, Phillips J, Scherer S, Cundiff P, DeBord K, Gilliland D, Hickman S, Jarvis A, Tong L, Ashby M. 1999. Comprehensive evaluation of isoprenoid biosynthesis regulation in *Saccharomyces cerevisiae* utilizing the genome reporter matrix. J Lipid Res 40:850–860.
45. Marada A, Allu PK, Murari A, PullaReddy B, Tammineni P, Thiriveedi VR, Danduprolu J, Sepuri NB. 2013. Mge1, a nucleotide exchange factor of Hsp70, acts as an oxidative sensor to regulate mitochondrial Hsp70 function. Mol Biol Cell 24:692–703. https://doi.org/10.1091/mbc.E12-10-0719.
46. Lussier M, White AM, Sheraton J, di Paolo T, Treadwell J, Southard SB, Horenstein CI, Chen-Weiner J, Ram AF, Kapteyn JC, Roemer TW, Vo DH, Bondoc DC, Hall J, Zhong WW, Sdicu AM, Davies J, Klis FM, Robbins PW, Bussey H. 1997. Large scale identification of genes involved in cell surface biosynthesis and architecture in *Saccharomyces cerevisiae*. Genetics 147:435–450.
47. Sakasegawa Y, Hachiya NS, Tsukita S, Kaneko K. 2003. Ecm10p localizes in yeast mitochondrial nucleoids and its overexpression induces extensive mitochondrial DNA aggregations. Biochem Biophys Res Commun 309:217–221. https://doi.org/10.1016/S0006-291X(03)01548-1.
48. Baumann F, Milisav I, Neupert W, Herrmann JM. 2000. Ecm10, a novel hsp70 homolog in the mitochondrial matrix of the yeast *Saccharomyces cerevisiae*. FEBS Lett 487:307–312. https://doi.org/10.1016/S0014-5793(00)02364-4.
49. Steger HF, Söllner T, Kiebler M, Dietmeier KA, Pfaller R, Trülzsch KS, Tropschug M, Neupert W, Pfanner N. 1990. Import of ADP/ATP carrier into mitochondria: two receptors act in parallel. J Cell Biol 111:2353–2363. https://doi.org/10.1083/jcb.111.6.2353.
50. Hines V, Brandt A, Griffiths G, Horstmann H, Brütsch H, Schatz G. 1990. Protein import into yeast mitochondria is accelerated by the outer membrane protein MAS70. EMBO J 9:3191–3200.
51. Dagley MJ, Gentle IE, Beilharz TH, Pettolino FA, Djordjevic JT, Lo TL, Uwamahoro N, Rupasinghe T, Tull DL, McConville M, Beaurepaire C, Nantel A, Lithgow T, Mitchell AP, Traven A. 2011. Cell wall integrity is linked to mitochondria and phospholipid homeostasis in *Candida albicans* through the activity of the post-transcriptional regulator Ccr4-Pop2. Mol Microbiol 79:968–989. https://doi.org/10.1111/j.1365-2958.2010.07503.x.
52. Kumánovics A, Chen OS, Li L, Bagley D, Adkins EM, Lin H, Dingra NN, Outten CE, Keller G, Winge D, Ward DM, Kaplan J. 2008. Identification of *FRA1* and *FRA2* as genes involved in regulating the yeast iron regulon in response to decreased mitochondrial iron-sulfur cluster synthesis. J Biol Chem 283:10276–10286. https://doi.org/10.1074/jbc.M801160200.
53. Perlroth J, Choi B, Spellberg B. 2007. Nosocomial fungal infections: epidemiology, diagnosis, and treatment. Med Mycol 45:321–346. https://doi.org/10.1080/13693780701218689.
54. Guinea J. 2014. Global trends in the distribution of *Candida* species causing candidemia. Clin Microbiol Infect 20(Suppl 6):5–10. https://doi.org/10.1111/1469-0691.12539.
55. Dujon B, Sherman D, Fischer G, Durrens P, Casaregola S, Lafontaine I, De Montigny J, Marck C, Neuvéglise C, Talla E, Goffard N, Frangeul L, Aigle M, Anthouard V, Babour A, Barbe V, Barnay S, Blanchin S, Beckerich JM, Beyne E, Bleykasten C, Boisramé A, Boyer J, Cattolico L, Confanioleri F, De Daruvar A, Despons L, Fabre E, Fairhead C, Ferry-Dumazet H, Groppi A, Hantraye F, Hennequin C, Jauniaux N, Joyet P, Kachouri R, Kerrest A, Koszul R, Lemaire M, Lesur I, Ma L, Muller H, Nicaud JM, Nikolski M, Oztas S, Ozier-Kalogeropoulos O, Pellenz S, Potier S, Richard GF, Straub ML. 2004. Genome evolution in yeasts. Nature 430:35–44. https://doi.org/10.1038/nature02579.
56. Skrzypek MS, Binkley J, Binkley G, Miyasato SR, Simison M, Sherlock G. 2017. The Candida Genome Database (CGD): incorporation of Assembly 22, systematic identifiers and visualization of high throughput sequencing data. Nucleic Acids Res 45:D592–D596. https://doi.org/10.1093/nar/gkw924.
57. Rodriguez-Tudela JL, Martinez-Suarez JV. 1994. Improved medium for fluconazole susceptibility testing of *Candida albicans*. Antimicrob Agents Chemother 38:45–48. https://doi.org/10.1128/AAC.38.1.45.
58. Murad AM, Lee PR, Broadbent ID, Barelle CJ, Brown AJ. 2000. Clp10, an efficient and convenient integrating vector for *Candida albicans*. Yeast 16:325–327.
59. Selmecki A, Forche A, Berman J. 2010. Genomic plasticity of the human fungal pathogen *Candida albicans*. Eukaryot Cell 9:991–1008. https://doi.org/10.1128/EC.00060-10.
60. Hallstrom TC, Moye-Rowley WS. 2000. Multiple signals from dysfunctional mitochondria activate the pleiotropic drug resistance pathway in *Saccharomyces cerevisiae*. J Biol Chem 275:37347–37356. https://doi.org/10.1074/jbc.M007338200.

61. Moczko M, Schönfisch B, Voos W, Pfanner N, Rassow J. 1995. The mitochondrial ClpB homolog Hsp78 cooperates with matrix Hsp70 in maintenance of mitochondrial function. J Mol Biol 254:538–543. https://doi.org/10.1006/jmbi.1995.0636.
62. Knight SA, Sepuri NB, Pain D, Dancis A. 1998. Mt-Hsp70 homolog, Ssc2p, required for maturation of yeast frataxin and mitochondrial iron homeostasis. J Biol Chem 273:18389–18393. https://doi.org/10.1074/jbc.273.29.18389.
63. Henneberry AL, Sturley SL. 2005. Sterol homeostasis in the budding yeast, *Saccharomyces cerevisiae*. Semin Cell Dev Biol 16:155–161. https://doi.org/10.1016/j.semcdb.2005.01.006.
64. Chen OS, Crisp RJ, Valachovic M, Bard M, Winge DR, Kaplan J. 2004. Transcription of the yeast iron regulon does not respond directly to iron but rather to iron-sulfur cluster biosynthesis. J Biol Chem 279:29513–29518. https://doi.org/10.1074/jbc.M403209200.
65. Puig S, Askeland E, Thiele DJ. 2005. Coordinated remodeling of cellular metabolism during iron deficiency through targeted mRNA degradation. Cell 120:99–110. https://doi.org/10.1016/j.cell.2004.11.032.
66. Kaplan J, McVey Ward D, Crisp RJ, Philpott CC. 2006. Iron-dependent metabolic remodeling in *S. cerevisiae*. Biochim Biophys Acta 1763:646–651. https://doi.org/10.1016/j.bbamcr.2006.03.008.
67. Schmidt S, Strub A, Röttgers K, Zufall N, Voos W. 2001. The two mitochondrial heat shock proteins 70, Ssc1 and Ssq1, compete for the cochaperone Mge1. J Mol Biol 313:13–26. https://doi.org/10.1006/jmbi.2001.5013.
68. Dong Y, Zhang D, Yu Q, Zhao Q, Xiao C, Zhang K, Jia C, Chen S, Zhang B, Zhang B, Li M. 2017. Loss of Ssq1 leads to mitochondrial dysfunction, activation of autophagy and cell cycle arrest due to iron overload triggered by mitochondrial iron-sulfur cluster assembly defects in *Candida albicans*. Int J Biochem Cell Biol 85:44–55. https://doi.org/10.1016/j.biocel.2017.01.021.
69. Schneider BL, Seufert W, Steiner B, Yang QH, Futcher AB. 1995. Use of polymerase chain reaction epitope tagging for protein tagging in *Saccharomyces cerevisiae*. Yeast 11:1265–1274. https://doi.org/10.1002/yea.320111306.
70. Fox TD, Folley LS, Mulero JJ, McMullin TW, Thorsness PE, Hedin LO, Costanzo MC. 1991. Analysis and manipulation of yeast mitochondrial genes. Methods Enzymol 194:149–165.
71. Janke C, Magiera MM, Rathfelder N, Taxis C, Reber S, Maekawa H, Moreno-Borchart A, Doenges G, Schwob E, Schiebel E, Knop M. 2004. A versatile toolbox for PCR-based tagging of yeast genes: new fluorescent proteins, more markers and promoter substitution cassettes. Yeast 21:947–962. https://doi.org/10.1002/yea.1142.
72. Swinnen E, Wilms T, Idkowiak-Baldys J, Smets B, De Snijder P, Accardo S, Ghillebert R, Thevissen K, Cammue B, De Vos D, Bielawski J, Hannun YA, Winderickx J. 2014. The protein kinase Sch9 is a key regulator of sphingolipid metabolism in *Saccharomyces cerevisiae*. Mol Biol Cell 25:196–211. https://doi.org/10.1091/mbc.E13-06-0340.
73. Kitada K, Yamaguchi E, Arisawa M. 1996. Isolation of a *Candida glabrata* centromere and its use in construction of plasmid vectors. Gene 175:105–108. https://doi.org/10.1016/0378-1119(96)00132-1.
74. Shen J, Guo W, Köhler JR. 2005. *CaNAT1*, a heterologous dominant selectable marker for transformation of *Candida albicans* and other pathogenic *Candida* species. Infect Immun 73:1239–1242. https://doi.org/10.1128/IAI.73.2.1239-1242.2005.
75. Sherman F. 2002. Getting started with yeast. Methods Enzymol 350:3–41. https://doi.org/10.1016/S0076-6879(02)50954-X.
76. Clinical and Laboratory Standards Institute. 2008. Reference method for broth dilution antifungal susceptibility testing of yeasts, 3rd ed. Approved standard. CLSI M27-A3 (28). Clinical and Laboratory Standards Institute, Wayne, PA.
77. Morio F, Pagniez F, Lacroix C, Miegeville M, Le Pape P. 2012. Amino acid substitutions in the *Candida albicans* sterol Delta5,6-desaturase (Erg3p) confer azole resistance: characterization of two novel mutants with impaired virulence. J Antimicrob Chemother 67:2131–2138. https://doi.org/10.1093/jac/dks186.
78. Müller C, Binder U, Bracher F, Giera M. 2017. Antifungal drug testing by combining minimal inhibitory concentration testing with target identification by gas chromatography-mass spectrometry. Nat Protoc 12:947–963. https://doi.org/10.1038/nprot.2017.005.
79. Hellemans J, Mortier G, De Paepe A, Speleman F, Vandesompele J. 2007. qBase relative quantification framework and software for management and automated analysis of real-time quantitative PCR data. Genome Biol 8:R19. https://doi.org/10.1186/gb-2007-8-2-r19.